Journal of
Applied Remote Sensing

Episodic deformation at Changbaishan Tianchi volcano, northeast China during 2004 to 2010, observed by persistent scatterer interferometric synthetic aperture radar

Lingyun Ji
Jiandong Xu
Qingliang Wang
Yuan Wan

SPIE

Episodic deformation at Changbaishan Tianchi volcano, northeast China during 2004 to 2010, observed by persistent scatterer interferometric synthetic aperture radar

Lingyun Ji,[a,b] Jiandong Xu,[a] Qingliang Wang,[b] and Yuan Wan[c]
[a]Institute of Geology, China Earthquake Administration, Key Laboratory of Active Tectonics and Volcano, Beijing 100029, China
dinsar010@hotmail.com
[b]China Earthquake Administration, Second Crust Monitoring and Application Center, Xi'an, Shaanxi 710054, China
[c]Institute of Geology, China Earthquake Administration, Beijing 100029, China

Abstract. Based on ENVISAT ASAR images taken from 2004 to 2010, we obtain the deformation time series of the Changbaishan Tianchi volcano by using persistent scatterer interferometric synthetic aperture radar (PSInSAR) technique. Then, the magma chamber parameters are derived by modeling the PSInSAR deformation field based on a Mogi point source. We draw the following conclusions. First, the magma chamber is located immediately beneath the caldera, with a depth of 9 km below sea level. Second, the Changbaishan Tianchi volcano inflated between August 2006 and August 2008, which may be a result of an episodic magma intrusion event leading to pressurization and a volume increase of the magma chamber. The deformation pattern changed oppositely during August 2008 to June 2010, with maximum subsidence more than 10 mm, which may be caused by magma cooling and crystallization in the crustal chamber. Moreover, the deformation fields consist of several components, including large-scale deformation caused by magmatic activity, the local deformation caused by the active faults, and others. In conclusion, our results indicate that the anomalous activity of the Changbaishan Tianchi volcano is obvious in recent years, providing a basis for further research on monitoring this active volcano to reduce hazards and risks of future eruptions. [DOI: 10.1117/1.JRS.7.073499]

Keywords: InSAR; PSInSAR; Changbaishan Tianchi volcano; volcano deformation; deformation modeling; volcano monitoring.

Paper 13194 received Jun. 3, 2013; revised manuscript received Aug. 26, 2013; accepted for publication Sep. 17, 2013; published online Oct. 4, 2013.

1 Introduction

The Changbaishan Tianchi volcano is a massive stratovolcano, located in the northeast of China, at the boundary between China and North Korea (Fig. 1). Based on the previous study, Changbaishan Tianchi volcano has experienced several stages of explosive eruption in history especially during the latest 1000 years, in which the 946 AD eruption, the so-called millennium eruption, is considered as one of the largest eruptions in the world in the past 2000 years.[1,2] At least three eruptive activities occurred in AD 1668, 1702, and 1903 after the millennium eruption.[3] Due to these large explosive eruption events, Changbaishan Tianchi volcano is considered the most dangerous volcano in China. From 2002 to 2006, volcanic seismicity, ground deformation, volcanic thermal anomaly, and volcanic gas geochemistry increased, indicating the volcano has begun to wake after more than 100 years of inactivity.[2,4,5] The 2002 to 2006 volcanic unrest events attracted much attention from the Chinese government and volcanologists.

Many researchers have used geophysical approaches to detect the magma system beneath the Changbaishan Tianchi volcano (e.g., see Refs. 6 and 7). Magnetotelluric soundings show that lower resistivity anomalies exist beneath the Changbaishan Tianchi volcano at a depth of 12 km.[6]

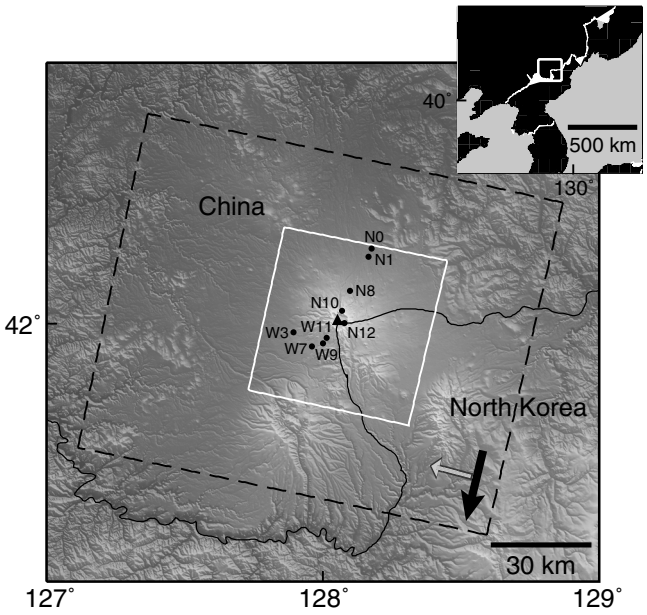

Fig. 1 Shaded relief map of Changbaishan Tianchi volcano and vicinity. Black dashed box outlines the ENVISAT SAR images. White solid box marks the area covered by interferograms shown in Figs. 3(a), 6. Black triangle denotes the location of Changbaishan Tianchi volcano. Black dots represent the leveling benchmarks. Satellite flight direction and radar look direction are labeled by black and white arrows, respectively. Inset shows the location of Changbaishan Tianchi volcano at the boundary between China and North Korea.

Seismic explosion experiments reveal that low-velocity anomalies in the crust and upper mantle are divided into three layers under the Changbaishan Tianchi volcano,[7] which is speculated to be the magma chamber. Thus, geophysical measurements indicate that the Changbaishan Tianchi volcano does have a magma chamber. However, the location and depth of the magma chamber from different approaches are different due to different spatial resolutions and other unknown reasons.

Geodetic measurements, including leveling and global positioning system (GPS) have also been carried out at the Changbaishan Tianchi volcano.[5,8,9] Hu et al.[8] modeled the leveling and GPS displacements based on a Mogi point source[10] in an elastic half space, and the result indicates that the magma chamber is located at a depth between 2 and 6 km beneath the caldera. Based on an ellipsoid point source model, Zhu et al.[11] made a jointly inversion using the leveling and GPS displacements, showing that the magma chamber is located in about 10 km depth. Obviously, different researchers got different magma chamber depths. These distinct results are probably related to those pointwise techniques, which cannot provide an adequately dense mapping of the deformation affecting the Changbaishan Tianchi volcano area.

Conventional interferometric synthetic aperture radar (InSAR) has proven to be an effective tool to study crustal deformation due to volcanic activities (e.g., see Refs. 12, 13, and 14). In contrast to leveling, GPS or other ground-based measurements, InSAR has the potential to dramatically improve the spatial density and continuity of surface displacement measurements. However, in Changbaishan Tianchi volcano area, heavy temporal decorrelation on the interferometric signal due to high vegetation coverage seriously limits the efficiency of the conventional InSAR approach (e.g., see Refs. 15 and 16). Besides, at Changbaishan Tianchi volcanic area, the accuracy of conventional InSAR measurements is also reduced by atmospheric artifacts that are difficult to remove from interferograms.[15] To overcome these limitations, we implement the Persistent scatterer interferometric synthetic aperture radar (PSInSAR) approach[17] to detect the crustal deformation around Changbaishan Tianchi volcano area. The PSInSAR technique considers those pixels that exhibit phase stability over a time series of interferograms, i.e., permanent or persistent scatterers. Hence, the PS pixels behave like point scatterers and interferometric decorrelation is greatly reduced. The PSInSAR technique has shown its potential for volcanic deformation monitoring worldwide (e.g., see Refs. 17, 18, 19, 20, and 21). In this article, we present

deformation time series during 2004 to 2010 around Changbaishan Tianchi volcano of the PSInSAR analysis based on a set of ENVISAT radar archives. To verify the accuracy of the PSInSAR-derived deformation, the precise leveling results are shown. Based on modeling, an interpretation of the displacement field observed at Changbaishan Tianchi volcano is proposed.

2 Dataset and PSInSAR Method

2.1 *Dataset*

To map the surface displacement associated with the volcanic activities, we use data from the ENVISAT SAR archive provided by the European Space Agency (ESA). Among all possible tracks covering the Changbaishan Tianchi volcano area, we focus on the descending track 146, which provides the largest number of suitable images for our analysis. We only choose SAR images acquired during the summer and early fall (from mid-May to mid-October) to avoid coherence loss due to snow and ice. Eighteen images (Table 1) acquired between May 2004 and June 2010 are selected at last.

2.2 *PSInSAR Method: StaMPS Processing*

We use the Stanford method for persistent scatterers (StaMPS) approach[19] to achieve the deformation time series. This approach has proven to be reliable even in natural terrains, especially in dense vegetated area. It does not rely on a prior assumption about the temporal nature of ground deformation. Instead, it assumes that the deformation and, consequently, the interferometric phase are spatially correlated.

Table 1 Parameters of ENVISAT ASAR images covered Changbaishan Tianchi volcanic area.

No.	Date	Orbit number	Fdc(Hz)
1	May 28, 2004	11723	163.65
2	July 2, 2004	12224	167.14
3	October 15, 2004	13727	159.78
4	June 17, 2005	17234	157.51
5	July 22, 2005	17735	159.06
6	August 26, 2005	18236	166.50
7	September 30, 2005	18737	185.55
8	June 2, 2006	22244	186.94
9	July 7, 2006	22745	183.43
10	August 11, 2006	23246	191.26
11	May 18, 2007	27254	177.27
12	July 17, 2007	28256	185.97
13	August 31, 2007	28757	190.98
14	August 15, 2008	33767	195.10
15	June 26, 2009	38276	189.49
16	July 31, 2009	38777	187.02
17	September 4, 2009	39278	186.87
18	June 11, 2010	43286	180.02

Table 2 Parameters used in the StaMPS processing.

Parameter	Value
DEM	SRTM 3 arc sec
Maximum DEM error	10 m
Band-pass phase filter grid cell size	20 m
Band-pass phase filter grid size	64×64
Band-pass phase filter low-pass cutoff	200 m
Band-pass phase filter α	1
Band-pass phase filter β	0.3
Spatially correlated filtering time window	730 days
Spatially correlated filtering minimum wavelength	200 m
Unwrapping algorithm	3-D
Unwrapping grid cell size	200 m
Unwrapping time window	365 days
Weed standard deviation	1.0
Reference range (longitude)	128.167–128.187
Reference range (latitude)	42.215–42.235

The main processing parameters are given in Table 2. A single reference (master) image acquired on June 17, 2005 is selected for the generation of interferogram stack. The resulting perpendicular baselines range between −900 and 710 m, whereas temporal baselines range between −385 and 1820 days (Fig. 2). Seventeen differential interferograms are generated with respect to the common master image using the conventional two-pass DInSAR approach (e.g., see Ref. 22). A digital elevation model from the Shuttle Radar Topography Mission (SRTM)[23] with 90-m pixel spacing is used to remove the topography phase from the interferograms. It is worth noting that we chose a strict threshold when selecting PS pixels, resulting in less false PS pixels that are included in the SAR interferograms. Also, this strict selection leads to sparse PS distribution (Fig. 3). The zero deformation area (i.e., reference area) is selected as the benchmark N0 of the Beipo leveling route (see Fig. 1 for location). Therefore, the two techniques, i.e., PSInSAR and leveling, have the same reference area. At the end of the StaMPS processing chain, the PS displacement time series at each acquisition date is reconstructed.

3 PSInSAR Results and Analysis

3.1 *PSInSAR Results*

The StaMPS processing identified a total of 7825 PS pixels in the study area (2490 km^2), with a mean point density of 3 PS/km^2 [Fig. 3(a)]. There are 13 PS pixels falling in the reference area [Fig. 3(b)]. Obviously, dense PS pixels are identified around the crater rim and the bare rock area at North Korea, whereas sparse PS pixels are identified around the volcano flank due to high vegetation coverage.

Figure 4 shows deformation time series of four certain PS pixels at Changbaishan Tianchi volcano. Time series are rescaled to the first acquisition (i.e., May 28, 2004), being understood that the PSInSAR master image (temporal reference) of the processing is the June 17, 2005, acquisition. Among the four PS pixels, one of them (i.e., N12) is located near the crater, and the other three are located at different parts of the volcano flank (Fig. 3). From the displacement time series map of the four PS pixels, we make the following observations (Fig. 4):

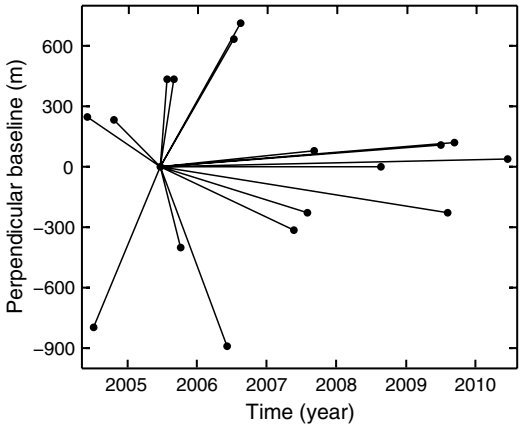

Fig. 2 Baseline plot for PS method. Dots represent SAR images and lines indicate the interferograms that are formed. The coordinates of the common master are taken as (0, 0).

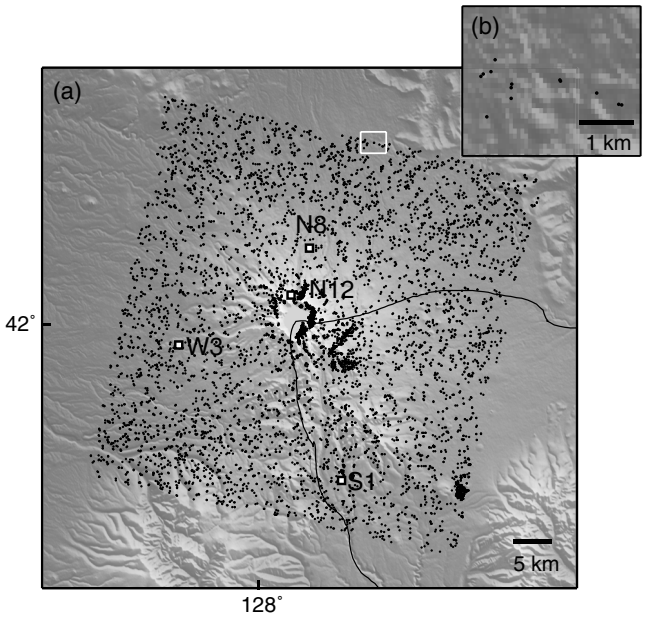

Fig. 3 (a) Distribution map of PS pixels at Changbaishan Tianchi volcano area. White box marks the reference area. White squares with black frame represent certain PS pixels, whose displacement time series are shown in Fig. 4. (b) shows the PS pixels distribution in the reference area.

1. Between May 2004 and August 2006, no significant deformation is observed in Changbaishan Tianchi volcano. In other words, deformation was generally lower than ± 5 mm during this period.
2. From August 2006 to August 2008, an inflation occurred at Changbaishan Tianchi volcano, with maximum displacement of 20 mm.
3. The deformation pattern changed to deflation from August 2008 to June 2010, with a nearly constant deformation rate. In other words, the subsidence that occurred in Changbaishan Tianchi volcano was linear with time during 2008 to 2010 with a total subsidence of 10 mm.

3.2 *Comparison with Leveling Results*

In order to evaluate the reliability of the PSInSAR measurements, the results should be compared with the deformation obtained from other techniques. From the GPS results shown in Ref. 5, the

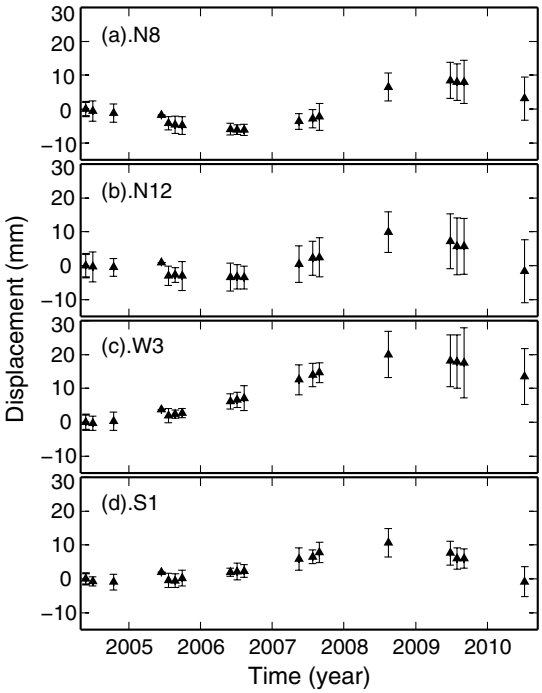

Fig. 4 Line of sight (LOS) displacement time series of certain pixels [see Fig. 3 for location; (a)–(b), (c), (d) are located on northern, western, and southern slope the edifice, respectively] at Changbaishan Tianchi volcano. Time series are rescaled to the first acquisition (i.e., May 28, 2004). Error bars are standard deviations estimated over the PS located within a certain radius. The minimum radius is set to 400 m. We increase it until at least 10 PS are found. The maximum radius is set to 3 km. If there are still less than 10 PS for such a maximum radius, the standard deviation will not be estimated.

horizontal displacements of Changbaishan Tianchi volcano were not significant at the 95% confidence level during 2004 and 2010, i.e., the PSInSAR-working period. Therefore, we assume that the ground displacement in Changbaishan Tianchi volcano occurs only in the vertical direction.

Thus, we compare the PSInSAR results against precise leveling results to quantitatively validate the results obtained. For the leveling results, the standard deviation of accidental error/km is 0.13 mm.[9] Based on the nearly vertical deformation assumption, the InSAR line of sight (LOS) measurements (d_{LOS}) can be converted to vertical displacements (d_v) following the relation $d_v = d_{\mathrm{LOS}}/\cos\theta$, where θ is incidence angle from the vertical. Eight benchmarks of precise leveling are chosen (see Fig. 1 for location). As the PS density is higher than the density of benchmarks, we estimate an average PS LOS displacement around each benchmark by selecting all PS pixels within a certain radius centered on each benchmark. The minimum radius is set to 400 m. We increase it until at least 10 PS pixels are found. The maximum radius is set to 3 km. Uncertainty of the average LOS displacement is estimated by the standard deviation of the individual PS LOS displacements inside this area.

The time series of vertical displacements show a good agreement between PSInSAR and leveling results (Fig. 5). Therefore, we conclude that PSInSAR can extract deformation with a high precision, even though the area is covered by dense vegetation. On the other hand, the agreement is consistent with our assumption of mainly vertical motion for the Changbaishan Tianchi volcano during 2004 to 2010.

3.3 *Modeling*

We assume that the surface deformation was caused by a volume change beneath the Changbaishan Tianchi volcano due to an injection or withdrawal of magmatic or hydrothermal

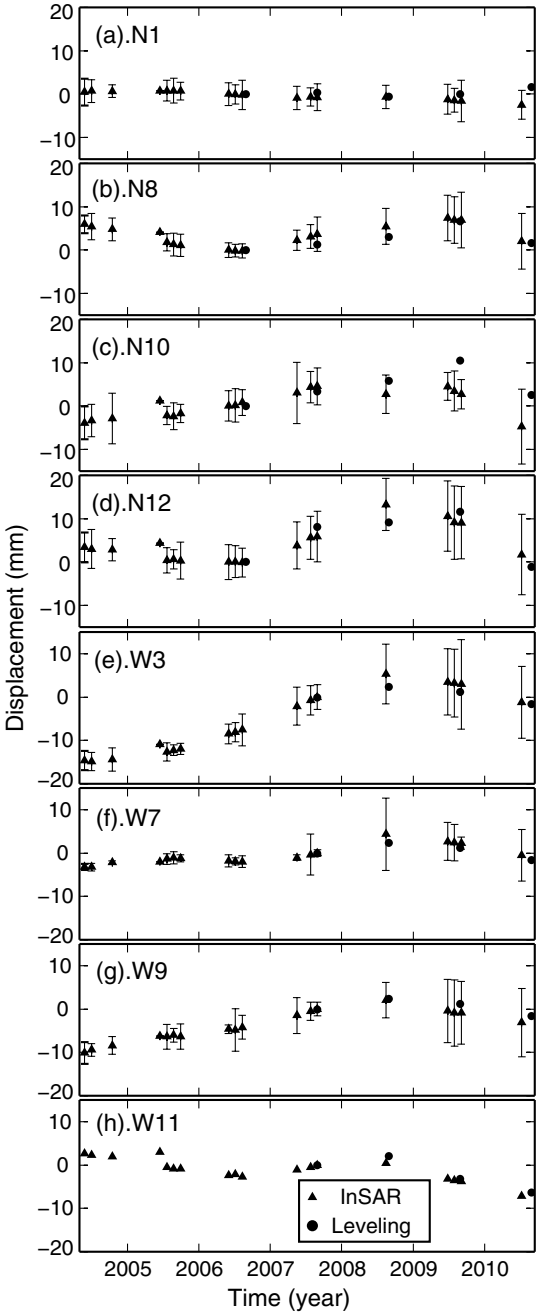

Fig. 5 Comparison of PSInSAR and leveling results. (a)–(d) and (e)–(h) show comparison results of Beipo and Xipo, respectively. Error bars are standard deviations, which are estimated using the same strategy in Fig. 4.

fluids. In order to explain the PSInSAR-detected deformation field, we test a point source of dilation in an elastic half-space[10] that includes a correction to account for topographic variation.[24] In the model, we introduce linear terms to account for any possible phase ramp due to uncertainties in satellite positions.[22] We use the downhill simplex method and Monte Carlo simulations[25] to estimate optimal parameters and their uncertainties, and the root mean square errors between the observed and modeled interferograms as the prediction-fit criterion. We choose the time series map obtained in August 2008 for modeling because this deformation map shows the largest inflationary displacement (Fig. 5). Figure 6(a) shows observed interferograms, Fig. 6(b) shows modeled interferograms, and Fig. 6(c) shows residual interferograms for the Mogi model. The cross shown in Fig. 6(b) represents the horizontal position of the

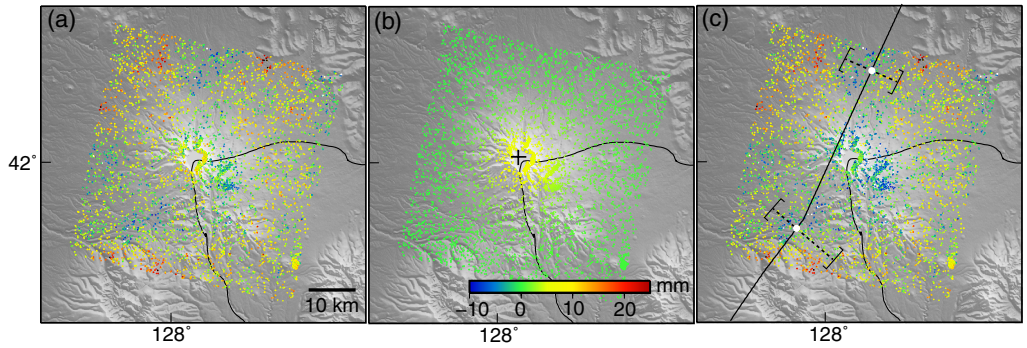

Fig. 6 Deformation modeling results. (a) observed map from PSInSAR, (b) modeled map from Mogi, (c) residual map. Cross shown in (b) represents the surface position of the best-fit Mogi source. Black solid line shown in (c) represents the Maanshan–Sandaobaihe fault (Ref. 26). Dashed lines are profiles with white circles indicating the origin of horizontal axes of plots shown in Fig. 8. Brackets show the sampling width for InSAR data.

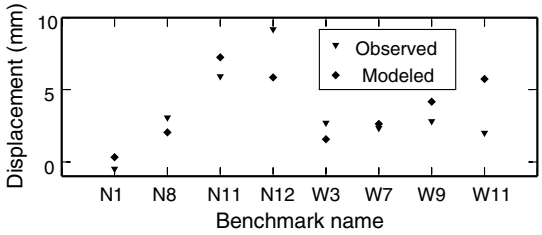

Fig. 7 Comparison between the forward modeled vertical deformation and the observed leveling results.

Mogi source. The Mogi source emplaced directly beneath the volcanic edifice of the Changbaishan Tianchi volcano, with a depth of 9-km below sea level. Then, we forward modeled the vertical deformation at the selected leveling benchmarks, based on the PSInSAR-inversed Mogi source. The observed and forward modeled displacements agree with each other reasonably well (Fig. 7), which indicates that the Mogi source can account for the magma chamber reasonably. However, in Fig. 6, the model cannot fit the observed interferogram very well according to the residual interferogram. All the model parameters are loosely constrained according to the uncertainties shown in Table 3. We will propose some possible explanations in Sec. 4.

4 Discussion

Our Mogi modeling test at Changbaishan Tianchi volcano indicates that the PSInSAR-derived deformation was caused by a Mogi point source centered about 9 km beneath the edifice.

Table 3 Parameters from Mogi source. Errors are in 95% confidence.

X (km)	-2.0 ± 2.1
Y (km)	-0.5 ± 1.5
Depth (km)	9.0 ± 2.6
Volume change (m^3)	$2.8 \times 10^6 \pm 1.1 \times 10^6$

Note: The reference for the horizontal coordinates (X, Y) is at (128.0559 deg, 42.0075 deg).

However, only the deformation around the caldera part can fit the observed one very well (Fig. 6). The large modeling residual may be caused by the following reasons, or combination of factors. First, the deformation is not large enough for modeling, even though we choose the largest accumulative deformation map. Second, the observed deformation might consist of several parts, for example, the deformation caused by magma recharge, local deformation, or noise. In other words, we speculate that only magma intrusion cannot account for the observed deformation. Next, we investigate the possible activities that occurred across the regional fault, i.e., Maanshan–Sandaobaihe fault [Fig. 6(c), fault trace is based on Ref. 26]. Figure 8 shows two profiles of LOS displacement across the Maanshan–Sandaobaihe fault. The two profiles reveal a slight change across the two sides of the fault, which may indicate that the fault was active during the study period. In addition, even though we chose a strict threshold when selecting PS pixels, there were some false PS pixels left, which may cause the large modeling residual.

According to the seismic record, a number of small volcano-tectonic earthquake swarms occurred at Changbaishan Tianchi volcano area.[27,28] Figure 9 shows the cumulative earthquake numbers during May 2004 to September 2010. Earthquake number increased gradually before 2008 and sporadic earthquakes occurred after 2008. These earthquake records and PSInSAR-derived deformation time series are particularly similar (Figs. 4 and 5). Generally, if there is no clear main shock for a volcano-tectonic swarm, the swarm may be triggered by a magmatic intrusion beneath the volcano.[29] Therefore, an episodic magma intrusion event may have occurred during August 2006 to August 2008. The intrusive magma went up along cracks in the shallow crust, which may perturb the stresses on overlaying faults, resulting earthquake swarms. The magma intrusion event ceased sometimes after August 2008, followed by a subsidence at the volcano, which may due to solidification of cooling magma or draining of magma.

Deformation accompanying seismicity has also been detected with InSAR at other volcanoes that have not erupted for more than a century, including Akutan volcano in Alaska and Campi Flegrei caldera in Italy. At Akutan, an intense seismic swarm occurred in March 1996,

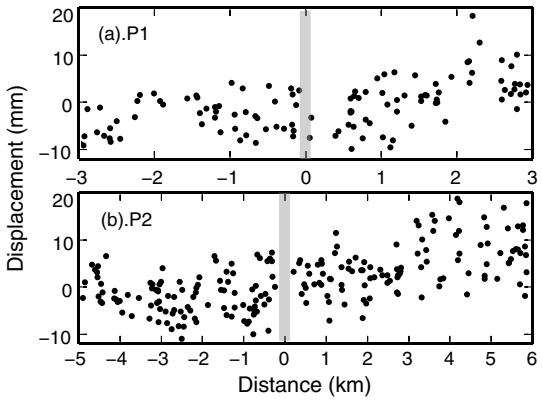

Fig. 8 Profiles P1 and P2, perpendicular to the Maanshan–Sandaobaihe fault, showing the displacement estimated from PSInSAR. Light gray boxes indicate the location of the Maanshan–Sandaobaihe fault.

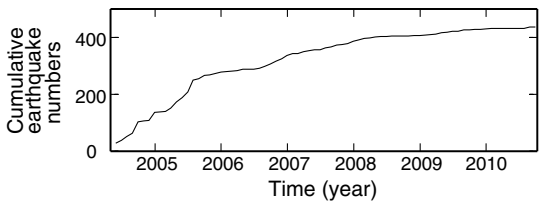

Fig. 9 Cumulative earthquake numbers from May 2004 to September 2010.

accompanying by as much as 60 cm of uplift on the western part of the island. However, no eruptive events issued during the seismicity active period.[30] The situation is similar at Campi Flegrei, where episodes of subsidence and uplift occurred during 1992 to 2006, accompanied by seismic activity, without producing eruptions.[31]

5 Conclusions

Using PSInSAR approach, we are able to extract the deformation time series at Changbaishan Tianchi volcano, even though it is covered by thick vegetation. Our modeling results show a Mogi point source at a depth of 9 km just beneath the caldera is responsible for the observed deformation. The modeling results indicate the deformation was not solely caused by magmatic activity. Active fault may produce a part of the observed deformation.

Changbaishan Tianchi volcano has produced multiple eruptions and pyroclastic flows in the past, and it is located close to densely populated areas, for example, Erdaobaihe county is located only 20 km from the Changbaishan Tianchi volcano. More than 60,000 inhabitants are directly at risk from the Changbaishan Tianchi volcano. We have presented results of PSInSAR time series survey of the Changbaishan Tianchi volcano from ENVISAT interferograms spanning 2004 to 2010. Such surveys are important for identifying deformation trends and deformed range, which can inform future hazard assessments.

Acknowledgments

We would like to thank two anonymous reviewers for comments that helped improve this manuscript. This research was supported by the special earthquake research project granted by the China Earthquake Administration (201208009), and Natural Science Foundation of Shanxi, China (2011021024-1). ENVISAT SAR data are copyrighted by ESA and were provided by ESA under CAT1-7864.

References

1. J. D. Xu et al., "Climatic impact of the millennium eruption of Changbaishan volcano in China: new insights from high-precision radiocarbon wiggle-match chronology," *Geophys. Res. Lett.* **40**(1), 54–59 (2013), http://dx.doi.org/10.1029/2012GL054246.
2. H. Q. Wei, G. M. Liu, and J. Gill, "Review of eruptive activity at Tianchi volcano, Changbaishan, northeast China: implications for possible future eruptions," *Bull. Volcanol.* **75**(4), 706–719 (2013), http://dx.doi.org/10.1007/s00445-013-0706-5.
3. R. X. Liu et al., "Volcano at Tianchi lake, Changbaishan—a modern volcano with potential danger of eruption," *Chin. J. Geophys.* **35**(5), 661–665 (1992), In Chinese with English abstract.
4. L. Y. Ji et al., "Application of satellite thermal infrared remote sensing in monitoring magmatic activity of Changbaishan Tianchi volcano," *Chin. Sci. Bull.* **55**(24), 2731–2737 (2010), http://dx.doi.org/10.1007/s11434-010-3232-2.
5. J. D. Xu et al., "Recent unrest of Changbaishan volcano, northeast China: a precursor of a future eruption?," *Geophys. Res. Lett.* **39**(16), L16305 (2012), http://dx.doi.org/10.1029/2012GL052600.
6. J. Tang et al., "Electric conductivity and magma chamber at the Tianchi volcano area in Changbaishan Mountain," *Seismo Geolo* **23**(2), 191–200 (2001), In Chinese with English abstract.
7. X. K. Zhang et al., "Deep seismic sounding investigation into the deep structure of the magma system in Changbaishan Tianchi volcanic region," *Acta Seismolog Sinica* **24**(2), 135–143 (2002), In Chinese with English abstract.
8. Y. X. Hu et al., "On active state of Changbaishan Tianchi volcano from deformation data," *J. Geodes. Geody.* **27**(5), 22–25 (2007), In Chinese with English abstract.
9. G. M. Liu, H. Y. Sun, and F. Guo, "The newest monitoring information of Changbaishan volcano, NE China," *Acta Petrologi Sinica* **27**(10), 2905–2911 (2011) (In Chinese with English abstract).

10. K. Mogi, "Relations between the eruptions of various volcanoes and the deformations of the ground surface around them," *Bull. Earthquake Res. Inst. Univ. Tokyo* **36**(2), 99–134 (1958).
11. G. Z. Zhu et al., "Modeling pressurized deformation source for Changbaishan volcano with homogenous expansion point source," *Chin. J. Geophys.* **51**(1), 108–115 (2008), In Chinese with English abstract.
12. L. Y. Ji et al., "Pre-eruption deformation caused by dike intrusion beneath Kizimen volcano, Kamchatka, Russia, observed by InSAR," *J. Volcanol. Geotherm. Res.* **256**(7), 87–95 (2013), http://dx.doi.org/10.1016/j.jvolgeores.2013.02.011.
13. Z. Lu, T. Masterlark, and D. Dzurisin, "Interferometric synthetic aperture radar study of Okmok volcano, Alaska, 1992–2003: Magma supply dynamics and postemplacement lava flow deformation," *J. Geophys. Res.* **110**(B2), B02403 (2005), http://dx.doi.org/10.1029/2004JB003148.
14. D. Massonnet, P. Briole, and A. Arnaud, "Deflation of Mount Etna monitored by spaceborne radar interferometry," *Nature* **375**(6532), 567–570 (1995), http://dx.doi.org/10.1038/375567a0.
15. Y. F. Han et al., "Deformation monitoring of Changbaishan Tianchi volcano using D-InSAR technique and error analysis," *Chin. J. Geophys.* **53**(7), 1571–1579 (2010), In Chinese with English abstract.
16. T. Ozawa and H. Taniguchi, "Detection of Crustal Deformation Associated with Volcanic Activity of Baitoushan Volcano Using SAR Interferometry," Vol. **71**, pp. 1–10, Report of National Research Institute for Earth Science and Disaster Prevention, Japan (2007), In Japanese with English abstract.
17. A. Hooper et al., "A new method for measuring deformation on volcanoes and other natural terrains using InSAR persistent scatterers," *Geophys. Res. Lett.* **31**(23), L23611 (2004), http://dx.doi.org/10.1029/2004GL021737.
18. M. P. Bato, A. A. Lagmay, and E. R. Paguican, "Interferometric SAR Persistent Scatterer Analysis of Mayon Volcano, Albay, Philippines," in *American Geophysical Union, Fall Meeting 2011*, abstract pp. G23A–0848 (2011).
19. A. Hooper, P. Segall, and H. Zebker, "Persistent scatterer InSAR for crustal deformation analysis, with application to Volcan Alcedo, Galapagos," *J. Geophys. Res.* **112**(B7), B07407 (2007), http://dx.doi.org/10.1029/2006JB004763.
20. Y. Miyagi et al., "DInSAR/PSInSAR observations of Kirishima, Shinmoe-dake Volcano, Japan. 15," EGU2013-4658-2 (2013).
21. A. Peltier et al., "PSInSAR as a new tool to monitor preeruptive volcano ground deformation: validation using GPS measurements on Piton de la Fournaise," *Geophys. Res. Lett.* **37**(12), L12301 (2010), http://dx.doi.org/10.1029/2010GL043846.
22. D. Massonnet and K. Feigl, "Radar interferometry and its application to changes in the Earth's surface," *Rev. Geophys.* **36**(4), 441–500 (1998), http://dx.doi.org/10.1029/97RG03139.
23. T. G. Farr and M. Kobrick, "Shuttle Radar Topography Mission produces a wealth of data," *EOS Trans. AGU* **81**(48), 583–585 (2000), http://dx.doi.org/10.1029/EO081i048p00583.
24. C. A. Williams and G. Wadge, "The effects of topography on magma chamber deformation models: application to Mt. Etna and radar interferometry," *Geophys. Res. Lett.* **25**(10), 1549–1552 (1998), http://dx.doi.org/10.1029/98GL01136.
25. W. Press et al., *Numerical recipes in C, the art of scientific computing*, pp. 994, Cambridge University Press, New York (1992).
26. Y. H. Duan et al., "Crystalline basement structure of Changbaishan Tianchi volcanic area," *Seismo Geolo* **25**(3), 501–508 (2003), In Chinese with English abstract.
27. J. P. Wu et al., "Seismic activity at the Changbaishan Tianchi volcano in the summer of 2002," *Chin. J. Geophys.* **48**(3), 621–628 (2005), In Chinese with English abstract.
28. J. P. Wu et al., "Earthquakes warm activity in Changbaishan Tianchi volcano," *Chin. J. Geophys.* **50**(4), 1089–1096 (2007), http://dx.doi.org/10.1002/cjg2.v50.4, In Chinese with English abstract.
29. Z. Lu et al., "Magmatic inflation at a dormant stratovolcano: 1996–1998 activity at Mount Peulik volcano, Alaska, revealed by satellite radar interferometry," *J. Geophys. Res.* **107**(B7), ETG4 (2002), http://dx.doi.org/10.1029/2001JB000471.

30. Z. Lu et al., "Surface deformation associated with the March 1996 earthquake swarm at Akutan Island, Alaska, revealed by C-band ERS and L-band JERS radar interferometry," *Canadian J. Rem. Sens.* **31**(1), 7–20 (2005), http://dx.doi.org/10.5589/m04-054.
31. G. Vilardo et al., "InSAR Permanent Scatterer analysis reveals fault reactivation during inflation and deflation episodes at Campi Flegrei caldera," *Rem. Sens. Environ.* **114**(10), 2373–2383 (2010), http://dx.doi.org/10.1016/j.rse.2010.05.014.

Lingyun Ji received his master degree in geodesy from Chang'an University in 2007 and the PhD degree in structural geology from Institute of Geology, China Earthquake Administration (CEA) in 2013. In July 2007, he joined the Second Crust Monitoring and Application Center, CEA, working on volcanic/seismic deformation using InSAR. He visited Cascades Volcano Observatory/USGS, as a visiting scientist from October 2011 to October 2012. His research interests concern InSAR applications, such as detecting volcanic/seismic deformation and modeling.

Jiandong Xu received his PhD degree from the University at Buffalo, the State University of New York in 1998. He is currently professor of Institute of Geology, CEA. His main research interests concern volcano geology, chronology, and volcanic activities monitoring.

Qingliang Wang received his PhD degree on geophysics from the Institute of Geophysics, CEA in 2003. He is currently the deputy director of the Second Crust Monitoring and Application Center, CEA, where he is professor of geophysics.

Yuan Wan received her PhD degree on structural geology from the Institute of Geology, CEA in 2012. Her research interests concern volcano geology, lahar, and mud volcanoes.